Materials Research Proceedings 41 (2024) 1190-1195 https://doi.org/10.21741/9781644903131-132

Inverse estimation of material model parameters using Bayesian data assimilation

YAMANAKA Akinori[1,a*], SUDA Michihiko[1,b], SUEKI Sae[1,c], SASAKI Kengo[1,d], and FUNAMOTO Ryuki[1,e]

[1]Tokyo University of Agriculture and Technology, 2-24-16, Naka-cho, Koganei, Tokyo, 184-8588, Japan

[a]a-yamana@cc.tuat.ac.jp, [b]s226270r@st.go.tuat.ac.jp, [c]s227904y@st.go.tuat.ac.jp, [d]s234450w@st.go.tuat.ac.jp, [e]s222036v@st.go.tuat.ac.jp

Keywords: Bayesian Data Assimilation, Digital Image Correlation, Material Model

Abstract. This study proposes a new method for the inverse estimation of the parameters included in material models from full-field measurement data that are obtained using the digital image correlation method. This approach is based on data assimilation according to the Bayes' theorem (Bayesian data assimilation). In this study, we demonstrate the assimilation of experimental data obtained from uniaxial tensile, forming, and fracture tests of aluminum alloys into elastoplastic finite element and phase-field crack propagation simulations. The proposed method allows the simultaneous estimation of multiple material model parameters. The Bayesian data assimilation is a promising methodology for estimating the parameters of different material models and constructing digital twins of material deformation.

Introduction

The sustainability in the development of newer products may be achieved by reducing the overall material consumption during the R&D of new devices. An effective approach to satisfy this requirement is constructing numerical simulation models that can quantitatively reproduce real phenomena in a virtual space, i.e., digital twins. However, the construction of digital twins requires accurate identification of the physical properties of target materials and the parameters included in material models that describe material behavior. The conventional methods for identifying material model parameters from experimental data include the virtual field method (VFM) [1] and the finite element model updating (FEMU) method [2, 3]. In recent years, inverse parameter estimation methods based on data assimilation (DA) and Bayes' theorem (Bayesian DA) have garnered considerable attention. The Bayesian DA algorithms can be classified into sequential and nonsequential. A representative example of the application of sequential DA in materials engineering is the ensemble Kalman filter, which has been applied to a phase-field model describing the evolution of microstructures in materials [4-6]. Furthermore, nonsequential DA has been applied to elastoplastic finite element (EPFE) simulations of the deformation and forming of metallic materials. In this study, we suggest the use of nonsequential DA to inversely estimate the material model parameters (i.e., parameters included in the constitutive equations, work-hardening laws, and yield functions) according to the full-field measurement data acquired using the digital image correlation (DIC) method. This paper presents the results of three case studies wherein nonsequential DA was applied to EPFE and phase-field crack (PFC) propagation simulations.

Bayesian DA

DA is based on the state–space model, which consists of a system model and an observation model expressed using the following equations [7]:

$$\boldsymbol{x}_t = M\left(\boldsymbol{x}_{t-1}\right) + \boldsymbol{v}_t, \tag{1}$$

where $\boldsymbol{x}_t$ is a state vector at time $t = n\Delta t$ (n = 1, 2, 3, …, N_{end}), which includes the state variables of the system and the material parameters to be estimated, M expresses the simulation model, and $\boldsymbol{v}_t$ is the system noise at time t, which corresponds to imperfections in the simulation model and numerical errors. The observational model is expressed as follows:

$$\boldsymbol{y}_t = H\left(\boldsymbol{x}_t\right) + \boldsymbol{w}_t. \tag{2}$$

Here, $\boldsymbol{y}_t$ is an observation vector that includes the experimental data obtained at time t. In this study, $\boldsymbol{y}_t$ contains the displacement and strain measured using the DIC method, H is an observation operator that extracts the components of $\boldsymbol{x}_t$ for comparison with those of $\boldsymbol{y}_t$, and $\boldsymbol{w}_t$ is the observational noise at time t, which shows the experimental errors.

DA tracks the evolution of the probability density function (PDF) $\boldsymbol{x}_t$ according to Eq. (1), and corrects the PDF based on Bayes' theorem, which is given using the following equation:

$$p\left(\boldsymbol{x}_t \middle| \boldsymbol{y}_{1:t}\right) = p\left(\boldsymbol{y}_t \middle| \boldsymbol{x}_t\right) p\left(\boldsymbol{x}_t \middle| \boldsymbol{y}_{1:t-1}\right). \tag{3}$$

Here, $p(\boldsymbol{x}_t \mid \boldsymbol{y}_{1:t-1})$, $p(\boldsymbol{y}_t \mid \boldsymbol{x}_t)$, and $p(\boldsymbol{x}_t \mid \boldsymbol{y}_{1:t})$ are the conditional PDFs referred to as the prior, likelihood, and posterior distributions, respectively. For example, $\boldsymbol{y}_{1:t-1}$ describes the observation data from time t = 1 to $t = (n-1)\Delta t$, where n is the number of time steps. It should be noted that all the PDFs in this study are assumed to be multivariate Gaussian functions.

The nonsequential DA is based on the four-dimensional variational method (4DVar). As shown in Fig. 1, the 4DVar searches the optimal state vector at time $t = 0$, $\boldsymbol{x}_0^{opt}$, which minimizes the cost function given by the following equation:

$$J\left(\boldsymbol{x}_0\right) = \frac{1}{2}(\boldsymbol{x}_0 - \boldsymbol{x}_0^b)^{\top}\boldsymbol{B}^{-1}(\boldsymbol{x}_0 - \boldsymbol{x}_0^b) + \sum_{t=0}^{t_{end}} \frac{1}{2}(H(\boldsymbol{x}_t) - \boldsymbol{y}_t)^{\top}\boldsymbol{R}_t^{-1}(H(\boldsymbol{x}_t) - \boldsymbol{y}_t) \tag{4}$$

The second term on the right-hand sides of Eq. (4) is the time integration of the misfit between the simulation and observation data (mathematically given by $H(\boldsymbol{x}_t) - \boldsymbol{y}_t$): $\boldsymbol{x}_0^b$ is a vector that contains the initially estimated system state and initial values of the parameters to be estimated. Further, $\boldsymbol{B}$ and $\boldsymbol{R}_t$ are the covariance matrices of $p(\boldsymbol{x}_0)$ and $p(\boldsymbol{w}_t)$, respectively.

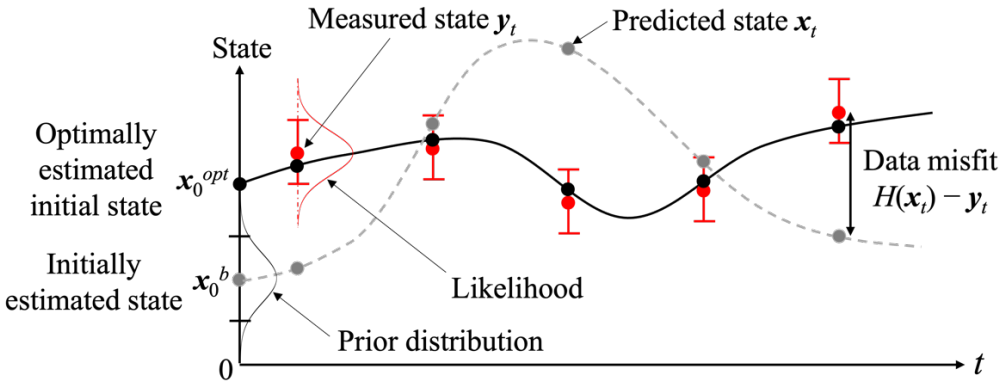

Figure 1 Schematic of 4DVar-based DA

To search for optimal state vector $\boldsymbol{x}_0^{opt}$, the conventional 4DVar calculates the gradient of the cost function, which is given by

$$\nabla J\left(\boldsymbol{x}_0\right) = \boldsymbol{B}^{-1}(\boldsymbol{x}_0 - \boldsymbol{x}_0^b) + \sum_{t=0}^{t_{end}} \hat{\boldsymbol{H}}_t^{\top}\boldsymbol{R}_t^{-1}(\hat{H}_t(\boldsymbol{x}_0) - \boldsymbol{y}_t), \tag{5}$$

where

$$\hat{H}_t(\boldsymbol{x}_0) = H(M^t(\boldsymbol{x}_0)) = \boldsymbol{H}_t \boldsymbol{M}_{t-1} \boldsymbol{M}_{t-2} \cdots \boldsymbol{M}_0. \quad (6)$$

To calculate Eq. (6), adjoint model $\boldsymbol{M}_t$ is required. $\boldsymbol{M}_t$ can be expressed as follows:

$$\boldsymbol{M}_t = \frac{\partial M(\boldsymbol{x}_t)}{\partial \boldsymbol{x}_t}. \quad (7)$$

However, the analytical derivation of $\boldsymbol{M}_t$ is difficult for nonlinear simulation models (e.g., the EPFE and PFC simulation models). Therefore, the ensemble 4DVar (En4DVar), which helps calculate the gradient of the cost function using the ensemble approximation of the PDF, has been used in previous studies [9, 10]. Furthermore, the DMC-TPE method [11] has been recently suggested for use as an adjoint model-free approach for 4DVar DA. The flowchart for estimating optimal state vector $\boldsymbol{x}_0^{opt}$ using the DMC-TPE method has been explained in a previous study [11].

Applications of Bayesian DA

This section presents the results of three case studies (I–III) using the En4DVar- and DMC-TPE-based DA methods. In case study I, En4DVar-based DA was used to estimate the parameters of the strain-hardening law according to the full-field measurement data of the uniaxial tensile test [12]. In this case study, a round bar specimen of the A5052-O aluminum alloy was used. MultiDIC [13] was used for full-field measurements of the displacement and strain fields at the specimen surface. The Hill'48 yield function and Swift's strain-hardening equation ($\sigma = C\left(\epsilon^p + \epsilon_0\right)^n$) were used for the EPFE simulation because this yield function and strain-hardening equation are widely adopted. The material models were implemented in ABAQUS/standard using UMMDp [14]. Parameters C, ϵ_0, and n in Swift's strain-hardening equation were targeted for estimation using En4DVar-based DA. The initial parameter estimates were assumed to follow a Gaussian PDF. The mean values of the initial estimates were C = 650 MPa, ϵ_0 = 0.0042, and n = 0.3, and the standard deviation was 10 % of the mean.

Figure 2(a) shows the variation in the cost function according to the number of iterative minimization calculations. Because the En4DVar minimizes the cost function based on the gradient of the cost function, the value of the cost function decreases monotonically. The optimal estimated values of the parameters that yielded the minimum value of the cost function were C = 320 MPa, ϵ_0 = 0.0053, and n = 0.113. By integrating the estimated parameters, the EPFE simulation reproduced the experimentally observed strain evolution, as shown in Fig. 2(b) and (c). A recent study demonstrated that En4DVar-based DA helps estimate not only the strain-hardening parameters but also the yield function parameters [15]. In future works, the estimated parameters can be compared with those identified using a classical analytical calibration method.

In case study II, DMC-TPE-based DA was used to estimate the parameters of the anisotropic yield function. To obtain the observational data, hole expansion tests and DIC measurements were performed on an A5052-O aluminum alloy sheet with a nominal thickness of 1.0 mm. In this study, we used the Yld2000-2d yield function, which describes the anisotropic plastic deformation behavior of the material. The parameters of the Yld2000-2d yield function were estimated from the full-field strain field data that were obtained using the DIC method. Furthermore, by integrating the estimated parameters, a deep-drawing test and an EPFE simulation were performed to verify the feasibility of the parameters. Figure 3(a) and (b) show the results of the deep-drawing simulation based on the estimated parameters and the experimentally obtained displacement distribution, respectively. It can be seen that the simulation qualitatively reproduces the experimentally measured displacement field. Figure 3(c) shows the absolute difference between the experimentally measured displacement field and simulation results. Although the simulation results slightly differ from the experimental results, the accuracy of the simulation may be improved by simultaneously estimating not only the yield function parameters but also the process parameters (e.g., the friction coefficient between the blank and punch).

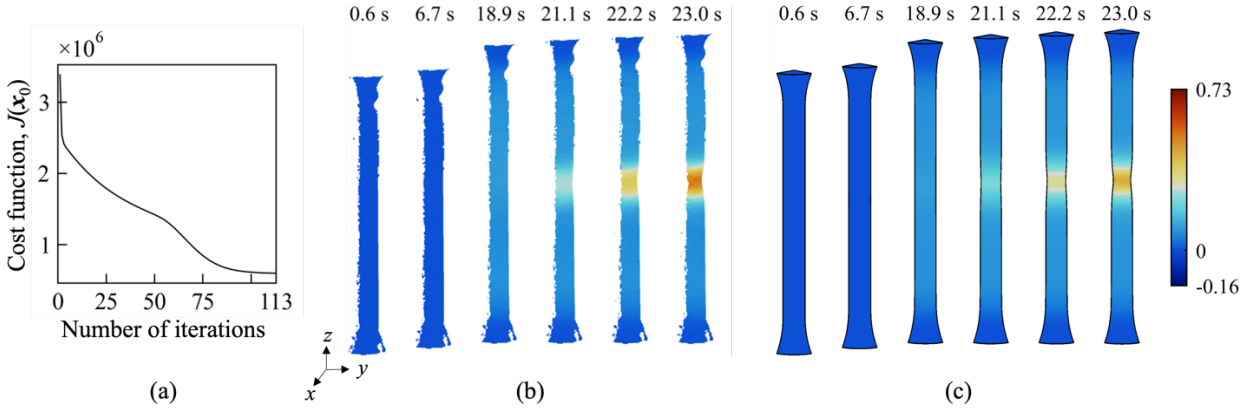

Figure 2 (a) Transition of cost function $J(\boldsymbol{x}_0)$. Evolution of strain ε_{zz} during uniaxial tensile deformation of the A5052-O aluminum alloy round bar specimen (b) measured by the DIC method and (c) simulated by the EPFE simulation with optimally estimated strain-hardening parameters.

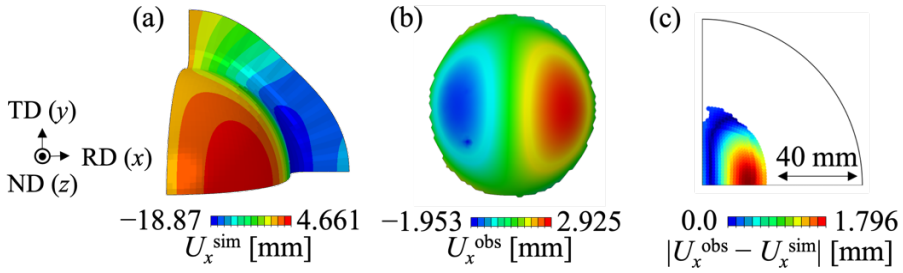

Figure 3 Distribution of displacement along x-direction (U_x) around the top of punch at a punch height of 60 mm (a) calculated using deep-drawing simulation with optimally estimated yield function parameters (U_x^{sim}) and (b) measured by the DIC method (U_x^{obs}). Absolute difference between simulated and measured displacements is shown in (c).

The PFC model is a numerical model that is suitable for simulating complex crack propagation behaviors, including crack branching and coarsening. In case study III, the parameters included in the PFC model, which represent the crack propagation behavior in sheet metals, were estimated using DA according to the DMC-TPE algorithm. A uniaxial tensile specimen was prepared from the same aluminum alloy sheet used in case study II. An asymmetrically notched specimen was fabricated to promote crack propagation. The crack propagation tests were performed at a tensile deformation rate ($\dot{U}$) of 2.0 mm/min.

The PFC model proposed by Khalil et al. [16] was used in this study. The model consists of the stress equilibrium equation and the governing equation of order parameter ϕ, as shown below:

$$(1-\phi)^2 \nabla \cdot \boldsymbol{\sigma} = 0, \tag{8}$$

where ϕ is the order parameter, which is defined as $\phi = 1$ inside a crack, and $\phi = 0$ inside an uncracked material. Here, ϕ changed smoothly from 0 to 1 at the diffusive interface between the cracked and uncracked domains. Further, $\boldsymbol{\sigma}$ denotes the Cauchy stress tensor. The governing equation for ϕ is as follows:

$$K\left(\frac{\phi}{l} - l\nabla^2\phi\right) - 2(1-\phi)\, g_{strain}(\boldsymbol{u}) = 0 \tag{9}$$

Here, K is a parameter related to the fracture toughness, l is a parameter that controls the thickness of the diffusive interface, $g_{strain}(\boldsymbol{u})$ is the strain energy, and $\boldsymbol{u}$ is the displacement vector.

For the crack propagation simulation using the PFC model, the weak forms of Eqs. (8) and (9) are solved using the FEM. In this study, the PFC model was implemented according to ABAQUS/Standard based on the user-defined subroutine UELMAT [16]. The plastic deformation of the specimens was analyzed using the von Mises yield function and Voce's strain-hardening equation:

$$\sigma = \sigma_0 + Q_\infty \left\{ 1 - \exp\left(-b\epsilon^p\right) \right\}. \tag{10}$$

Here, σ_0, Q_∞, and b are the strain-hardening parameters. In case study III, the four parameters (i.e., K, σ_0, Q_∞ and b) were estimated from the full-field strain field data by DMC-TPE-based DA. The initial estimates of the parameters were K = 500 kJ/mm^2, σ_0 = 87.2 MPa, Q_∞ = 165.6 MPa, and b = 15.5.

After the minimization of the cost function, the optimally estimated parameters included in vector $\boldsymbol{x}_0^{opt}$ were K = 472.9 kJ/mm^2, σ_0 = 94.37 MPa, Q_∞ = 295.85 MPa, and b = 9.68. The computation time required to obtain the optimally estimated parameters was approximately 35 h without parallel computing. Figure 4(a) shows the evolution of true strain ε_{yy} measured using the DIC method as the cracks propagated. It can be observed that the strain concentration occurs near the crack tip as forced displacement U increased along the y direction. Figure 4(b) shows the crack propagation behavior (i.e., time evolution of ϕ) obtained from the PFC simulation using the optimally estimated parameters. It is evident that the PFC simulation reproduces a crack propagation behavior similar to that observed in the experiment.

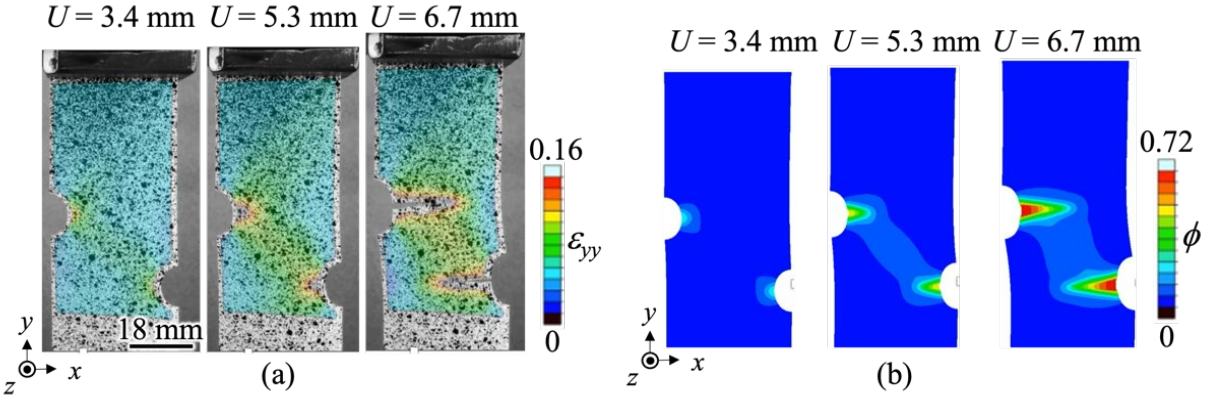

Figure 4 Evolution of (a) true strain ε_{yy} during the crack propagation measured using the DIC method and (b) order parameter ϕ describing the crack propagation behavior simulated by the PFC model with optimally estimated parameters.

Summary

This paper presents the results of three case studies wherein Bayesian DA methods were applied to the deformation (case study I), formation (case study II), and fracture (case study III) of the A5052-O aluminum alloy. The results show that Bayesian DA is an effective tool for estimating the parameters of material models by utilizing full-field measurement data from the DIC method, which contributes to the digital twin construction of each phenomenon.

Acknowledgement

This research was financially supported by the Japan Society for the Promotion of Science Grant-in-Aid for Scientific Research (KAKENHI) (B) (Grant Numbers: 20H02476 and 23H01297) and the AMADA Foundation (Grant Number: AF-2021002-A2).

References

[1] M. Grédiac, E. Toussaint, F. Pierron, Special virtual fields for the direct determination of

material parameters with the virtual fields method. 2—Application to in-plane properties, Int. J. Solids Struct. 39 (2002) 2707-2730. https://doi.org/10.1016/S0020-7683(02)00128-2
[2] K.T. Kavanagh, R.W. Clough, Finite element applications in the characterization of elastic solids, Int. J. Solids Struct. 7 (1971) 11-23. https://doi.org/10.1016/0020-7683(71)90015-1
[3] Y. Zhang, A. Yamanaka, S. Cooreman, T. Kuwabara, S. Coppieters, Inverse identification of plastic anisotropy through multiple non-conventional mechanical experiments, International Journal of Solids and Structures, Vol. 285 (2023) 112534. https://doi.org/10.1016/j.ijsolstr.2023.112534
[4] K. Sasaki, A. Yamanaka, S. Ito, H. Nagao, Data Assimilation for Phase-field Models based on the Ensemble Kalman Filter, Comput. Mater. Sci., 141 (2018) 141-152. https://doi.org/10.1016/j.commatsci.2017.09.025
[5] A. Yamanaka, Y. Maeda, K. Sasaki, Ensemble Kalman filter-based data assimilation for three-dimensional multi-phase-field model: Estimation of anisotropic grain boundary properties, Mater. Design, 165, (2019), 107577. https://doi.org/10.1016/j.matdes.2018.107577
[6] K. Takahashi, A. Yamanaka, Quantitative three-dimensional phase-field modeling of dendritic solidification coupled with local ensemble transform Kalman filter, Comput. Mater. Sci., 190 (2021) 110296. https://doi.org/10.1016/j.commatsci.2021.110296
[7] W. Lahoz, B. Khattatov, R. Ménard, Data Assimilation: Making Sense of Observations, Springer, Germany, 2010. https://doi.org/10.1007/978-3-540-74703-1
[8] G. Evensen, Sequential data assimilation with a nonlinear quasi-geostrophic model using Monte Carlo methods to forecast error statistics, J. Geophys. Res. Oceans, 99 (1994) 10143-10162. https://doi.org/10.1029/94JC00572
[9] A. Ishii, A. Yamanaka, Y. Okada, A. Yamamoto, Estimation of solid-state sintering and material parameters using phase-field modeling and ensemble four-dimensional variational method, Model. Simul. Mater. Sci. Eng., 29 (2021) 065012. https://doi.org/10.1088/1361-651X/ac13cd
[10] S. Sueki, A. Ishii, S. Coppieters, A. Yamanaka, Inverse characterization of a material model using an ensemble-based four-dimensional variational method, Int. J. Solids Struct., 279 (2023) 112350. https://doi.org/10.1016/j.ijsolstr.2023.112350
[11] A. Ishii, A. Yamamoto, A. Yamanaka, DMC-TPE: Tree-Structured Parzen Estimator-Based Efficient Data Assimilation Method for Phase-Field Simulation of Solid-State Sintering, *Sci. Technol. Adv. Mater. Methods*, 3 (2023) 2239133 https://doi.org/10.1080/27660400.2023.2239133
[12] S. Sueki, A. Ishii and A. Yamanaka, Bayesian data assimilation for inverse material modelling using 3D-digital image correlation measurement, Proceedings of JSME International Conference on Materials and Processing 2022, Paper #Tu-3B-3.
[13] D. Solav, K.M. Moerman, A.M. Jaeger, K. Genovese, H.M. Herr, IEEE Access, 6 (2018) 30520-30535. https://doi.org/10.1109/ACCESS.2018.2843725
[14] H. Takizawa, T. Kuwabara, K. Oide, J. Yoshida, Development of the subroutine library 'UMMDp' for anisotropic yield function commonly applicable to commercial FEM codes, J. Phys. Conf. Ser., 734 (2016), 032028. https://doi.org/10.1088/1742-6596/734/3/032028
[15] S. Sueki, A. Ishii, A. Yamanaka, Inverse Estimation of Material Model Parameters Using Digital Image Correlation and Ensemble-based Four-dimensional Variational Methods, J. Jpn. Soc. Technol. Plast., 64 (2023) 195-201. https://doi.org/10.9773/sosei.64.195
[16] Z. Khalil, A.Y. Elghazouli, E. Martínez-Pañeda, A generalised phase field model for fatigue crack growth in elastic-plastic solids with an efficient monolithic solver, Comput. Methods Appl. Mech. Eng., 388 (2022) 114286. http://dx.doi.org/10.1016/j.cma.2021.114286